

Physical parameters of the high-mass X-ray binary 4U1700-37^{*}

J. S. Clark¹, S. P. Goodwin², P. A. Crowther¹, L. Kaper³, M. Fairbairn⁴, N. Langer⁵, and C. Brocksopp⁶

¹ Department of Physics and Astronomy, University College London, Gower Street, London, WC1E 6BT, England, UK

² Department of Physics and Astronomy, University of Wales, Cardiff, CF24 3YB, Wales, UK

³ Astronomical Institute “Anton Pannekoek”, University of Amsterdam and Center for High-Energy Astrophysics, Kruislaan 403, 1098 SJ Amsterdam, The Netherlands

⁴ Service de Physique Théorique, CP225, Université Libre de Bruxelles, 1050 Brussels, Belgium

⁵ Astronomical Institute, Utrecht University, Princetonplein 5, 3584 CC, Utrecht, The Netherlands

⁶ Astrophysics Research Institute, Liverpool John Moores University, Liverpool, L41 1LD, UK

Received 22 March 2002 / Accepted 20 June 2002

Abstract. We present the results of a detailed non-LTE analysis of the ultraviolet and optical spectrum of the O6.5 Iaf⁺ star HD 153919 – the mass donor in the high-mass X-ray binary 4U1700-37. We find that the star has a luminosity $\log(L_*/L_\odot) = 5.82 \pm 0.07$, $T_{\text{eff}} = 35\,000 \pm 1000$ K, radius $R_* = 21.9_{-0.5}^{+1.3} R_\odot$, mass-loss rate $\dot{M} = 9.5 \times 10^{-6} M_\odot \text{ yr}^{-1}$, and a significant overabundance of nitrogen (and possibly carbon) relative to solar values. Given the eclipsing nature of the system these results allow us to determine the most likely masses of both components of the binary via Monte Carlo simulations. These suggest a mass for HD 153919 of $M_* = 58 \pm 11 M_\odot$ – implying the initial mass of the companion was rather high ($\geq 60 M_\odot$). The most likely mass for the compact companion is found to be $M_x = 2.44 \pm 0.27 M_\odot$, with only 3.5 per cent of the trials resulting in a mass less than $2.0 M_\odot$ and none less than $1.65 M_\odot$. Such a value is significantly in excess of the upper observational limit to the masses of neutron stars of $1.45 M_\odot$ found by Thorsett & Chakrabarty (1999), although a mass of $1.86 M_\odot$ has recently been reported for the Vela X-1 pulsar (Barziv et al. 2001). Our observational data is inconsistent with the canonical neutron star mass and the lowest black hole mass observed ($\geq 4.4 M_\odot$; Nova Vel). Significantly changing observational parameters *can* force the compact object mass into either of these regimes but, given the strong proportionality between M_* and M_x , the O-star mass changes by factors of greater than 2, well beyond the limits determined from its evolutionary state and surface gravity. The low mass of the compact object implies that it is difficult to form high mass black holes through both the Case A & B mass transfer channels and, if the compact object is a neutron star, would significantly constrain the high density nuclear equation of state.

Key words. stars: early-type – stars: individual: HD153919, 4U1700-37 – X-rays: stars – stars: binaries: general

1. Introduction

First detected by the *Uhuru* satellite (Jones et al. 1973) the eclipsing X-ray source 4U 1700-37 was quickly associated with the luminous O6.5 Iaf⁺ star HD 153919, confirming 4U 1700-37 as a high-mass X-ray binary (henceforth HMXB). HMXBs are systems composed of an OB star and a compact companion (neutron star or black hole), with the X-ray emission resulting from the accretion of material by the compact companion. In the subclass of supergiant HMXB systems material is accreted either via Roche lobe overflow or directly from the powerful stellar wind of the OB primary. Given that HD 153919 slightly underfills its Roche Lobe (e.g. Conti 1978) mass transfer proceeds via the latter mechanism.

Although an orbital period of ~ 3.412 days (Jones et al. 1973) was quickly identified for 4U 1700-37, extensive searches (e.g. Rubin et al. 1996 and references therein) have

failed to identify any other X-ray periodicities within the system that might correspond to the pulse period for a possible neutron star (although König & Maisack 1997 claim the presence of a 13.81 day period in CGRO BATSE & RXTE ASM datasets). Given the absence of any X-ray pulsations and the unusually hard nature of the spectrum various authors (e.g. Brown et al. 1996) have suggested that the compact companion could be a low mass black hole rather than a neutron star. However, Reynolds et al. (1999) point out that the 2–200 keV spectrum of 4U 1700-37 differs from those commonly observed for black hole candidates such as Cygnus X-1. Given that the X-ray spectrum of 4U 1700-37 is qualitatively similar to those of accreting neutron stars they suggest that the compact object is also a neutron star, and explain the lack of pulsations as due to either a weak magnetic field or an alignment of the magnetic field with the spin axis.

With a spectral type of O6.5 Iaf⁺, HD 153919 is the hottest and potentially most massive mass donor of any of the the HMXB systems. As such, determination of its fundamental parameters (radius, temperature, mass and chemical composition) is of importance given that these will potentially provide

Send offprint requests to: J. S. Clark,

e-mail: jsc@star.ucl.ac.uk

^{*} Based on observations collected at the European Southern Observatory, La Silla, Chile (64.H-0224).

valuable insights into the evolution of very massive stars and their ultimate fate. In particular by determining the masses of the components of HMXB systems, limits to the progenitor masses for neutron stars and black holes in such systems can be found¹ while the chemical composition of the mass donor can shed light on the pre-supernova (SN) mass transfer mechanisms.

The paper is ordered as follows. Section 2 describes the determination of the physical properties of HD 153919; the complete dataset and the non-Local Thermal Equilibrium (non-LTE) code used to analyse it. Section 3 describes the Monte-Carlo technique used to determine the masses of both components of the binary system. In Sects. 4 and 5 we discuss the implications of our results for the evolution of hot massive stars, limits for the progenitor masses of compact objects and the equation of state for nuclear matter. Finally in Sect. 6 we summarize the main results of the paper.

2. Determination of the stellar parameters for HD 153919

Determination of the fundamental stellar parameters of HD 153919 is complicated by its high temperature and mass loss rate, which necessitates a sophisticated non-LTE treatment. Early attempts to determine the physical properties of HD 153919 suggested that the star might be undermassive by a factor of 2 (e.g. Conti 1978; Hutchings 1974) which would imply that the terminal velocity of the stellar wind ($V_\infty \sim 1700 \text{ km s}^{-1}$; van Loon et al. 2001, henceforth vL01) is a factor of 10 in excess of the escape velocity (V_{esc}). Given that Howarth & Prinja (1997) show that $V_\infty/V_{\text{esc}} < 4$ for O stars (and typically ~ 2.5) this discrepancy clearly needs to be resolved. More recent analyses still do not resolve the issue, with Heap & Corcoran (1992) suggesting a mass for HD 153919 of $M_* = 52 \pm 2 M_\odot$ (thus broadly in line with the expected mass for such a star) while Rubin et al. (1996) propose $M_* = 30_{-7}^{+11} M_\odot$, suggesting that the star is probably undermassive for its spectral type.

As will be shown in Sect. 3, determination of the masses of *both* components in the system is hampered by the considerable uncertainties in the stellar radius of HD 153919. In order to address this problem, and in the light of dramatic advances in the sophistication of non-LTE model atmospheres we have decided to reanalyse both new and published ultraviolet to near-infrared spectroscopic and optical to mid-infrared photometric observations of HD 153919 in order to refine previous estimates of the stellar parameters.

2.1. The complete dataset

Archival and new ultraviolet to mid-infrared spectroscopic and photometric data were used to derive a set of stellar parameters for HD 153919. High spectral resolution UV spectroscopy was obtained with the *International Ultraviolet Explorer* (IUE); the data used and reduction procedures employed are described

in Kaper et al. (1993); the details are not repeated here. Four high S/N and high spectral resolution ($R = 48\,000$) optical spectra ($\sim 3700\text{--}8600 \text{ \AA}$) were obtained in 1999 April with the Fiber-fed Extended Range Optical Spectrograph (FEROS) mounted on the ESO 1.52 m telescope at La Silla. All 4 spectra were wavelength calibrated and optimally extracted to determine if significant changes in the spectrum occurred at different orbital periods. Besides line-profile variability in the strongest “wind” lines and the shift in radial velocity due to orbital motion, no evidence is found for intrinsic variability of the photospheric spectrum. The final spectrum used for determining the stellar parameters of HD 153919 was that taken during X-ray eclipse to further minimize the effects of any perturbation of the wind by the presence of the compact companion (see Sect. 2.2). Near-infrared spectra between $1\text{--}2.2 \mu\text{m}$ and optical to near-infrared photometry were taken from Bohannan & Crowther (1999) and mid-IR photometry ($6.8 \mu\text{m} = 669 \text{ mJy}$, $11.5 \mu\text{m} = 244 \text{ mJy}$) from Kaper et al. (1997); see respective papers for the particular reduction strategies employed in each case.

2.2. Spectral analysis

To determine the stellar properties of HD 153919 we have utilised the non-LTE code of Hillier & Miller (1998) which solves the radiative transfer equation subject to the constraints of statistical and radiative equilibrium, in a spherical, extended atmosphere. Line blanketing is incorporated directly through the use of a super-level approach. We use a similar atomic model to that employed by Crowther et al. (2002) in their study of early O supergiants, including H I, He I-II, C III-IV, N III-V, O III-VI, Si IV, P IV-V, S IV-VI and Fe IV-VII. For extreme O supergiants, line blanketing and the strong stellar wind conspire to produce significant differences in stellar parameters relative to the standard plane-parallel hydrostatic results (see Crowther et al. 2002 for further details).

Our procedure is as follows. We adjust the stellar temperature² and mass-loss rate of an individual model until the “photospheric” He II $\lambda 4542$ and He I $\lambda 4471$ lines are reproduced. Simultaneously, we vary the total mass-loss rate until H α is also matched. The exponent of the β -law is adjusted until the shape of H α is well reproduced – for HD 153919 we obtain $\beta \sim 1.3$. The input atmospheric structure, connecting the spherically extended hydrostatic layers to the β -law wind is achieved via a parameterized scale height, h (see Hillier et al. 2002 for details), for which $h = 0.001$ yields a reasonable match to He I and Balmer line wings, consistent with $\log g = 3.45\text{--}3.55$. We adopt a terminal wind velocity of $v_\infty = 1750 \text{ km s}^{-1}$ (vL01; Howarth et al. 1997).

The formal solution of the radiative transfer equation yielding the final emergent spectrum is computed separately, and includes standard Stark broadening tables for H I, He I-II. Except where noted, these calculations assume a microturbulent velocity $v_{\text{turb}} = 10 \text{ km s}^{-1}$. Hillier et al. (2002) also discuss the

¹ We note that Wellstein & Langer (1999) demonstrate that such limits derived from binary systems cannot be *directly* applied to single stars.

² Defined, as is usual for an extended atmosphere, as the effective temperature corresponding to the radius at a Rosseland optical depth of 20.

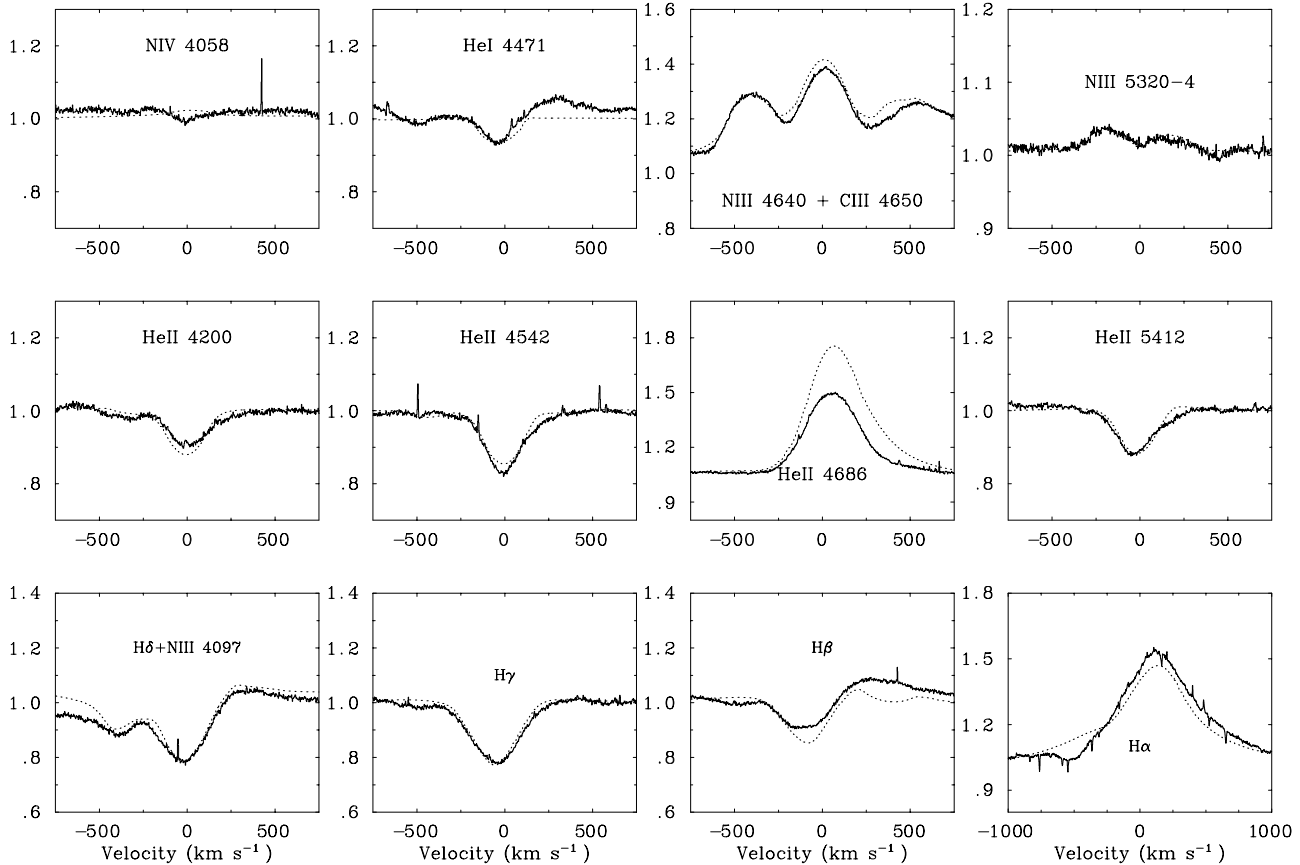


Fig. 1. Plots of selected regions of the optical spectrum of HD 153919 (solid line) and best fit model (dotted line); parameters listed in Table 1.

effect of varying v_{turb} in O star models. Additionally, we find good agreement with observations using $v \sin i = 150 \text{ km s}^{-1}$ (Howarth et al. 1997 derived 120 km s^{-1}).

It is extremely difficult to determine accurate He/H abundances in O supergiants as discussed by Hillier et al. (2002). Consequently, we adopt $\text{He}/\text{H} = 0.2$ by number, whilst C and N abundances are varied until diagnostic optical line profiles are reproduced. In Fig. 1 we present selected optical line profile fits to FEROS observations of HD 153919. Overall, agreement for $T_{\text{eff}} = 35 \text{ kK}$ is very good, with the exception of He II $\lambda 4686$. He I $\lambda 4471$ provides our main temperature constraint since other blue optical He I lines are weak or absent. Alternatively, we considered using He I $\lambda 5876$ (or $\lambda 10830$) together with the He II $\lambda 4686$ line. However, this method (followed by Crowther & Bohannan 1997) yields significantly ($\sim 4 \text{ kK}$) lower stellar temperatures, and suffers from inconsistencies involving the ionization balance of UV/optical metal lines. Therefore, we have greater confidence in our adopted diagnostics, which do not suffer from such problems.

From spectral energy distribution fits to IUE spectrophotometry and Johnson photometry (Fig. 2), we derive $E_{B-V} = 0.53 \pm 0.02 \text{ mag}$. Alternatively, using the intrinsic colour of $(B - V)_0 = -0.30$ from the early O supergiant calibration of Schmidt-Kaler (1982), we derive $E_{B-V} = 0.55$ from Johnson photometry of HD 153919 ($V = 6.54$ and $B - V = 0.25$, Bolton & Herbst 1976). Consequently, we adopt $E_{B-V} = 0.54 \pm 0.02$ for the remainder of this work. We adopt a distance

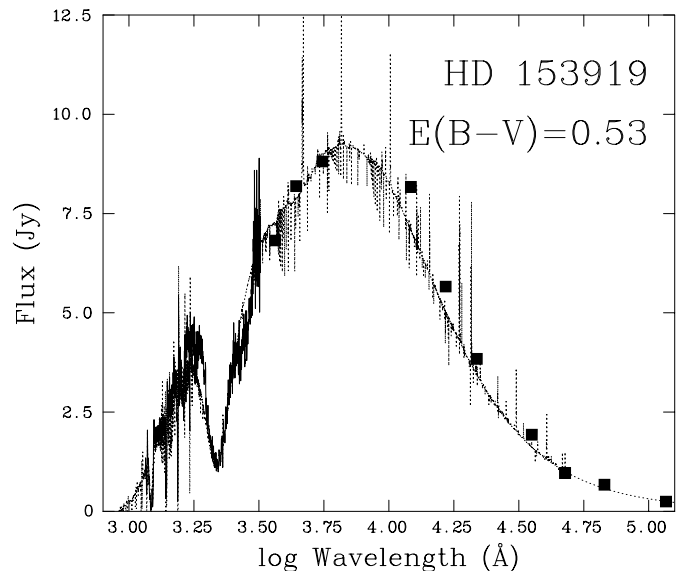


Fig. 2. Plot of the observed (solid line and data points) and theoretical (dotted line) UV-mid-IR spectral energy distribution for HD 153919.

modulus of 11.4 mag to HD 153919 (Ankay et al. 2001), implying $M_V = -6.53 \text{ mag}$. Our derived temperature provides a bolometric correction of -3.3 mag , therefore we obtain $\log(L/L_\odot) = 5.82$ for HD 153919, and thus $R = 21.9 R_\odot$. The derived mass-loss rate is $9.5 \times 10^{-6} M_\odot \text{ yr}^{-1}$, assuming that the H α line-forming region is not clumped. Moderate clumping

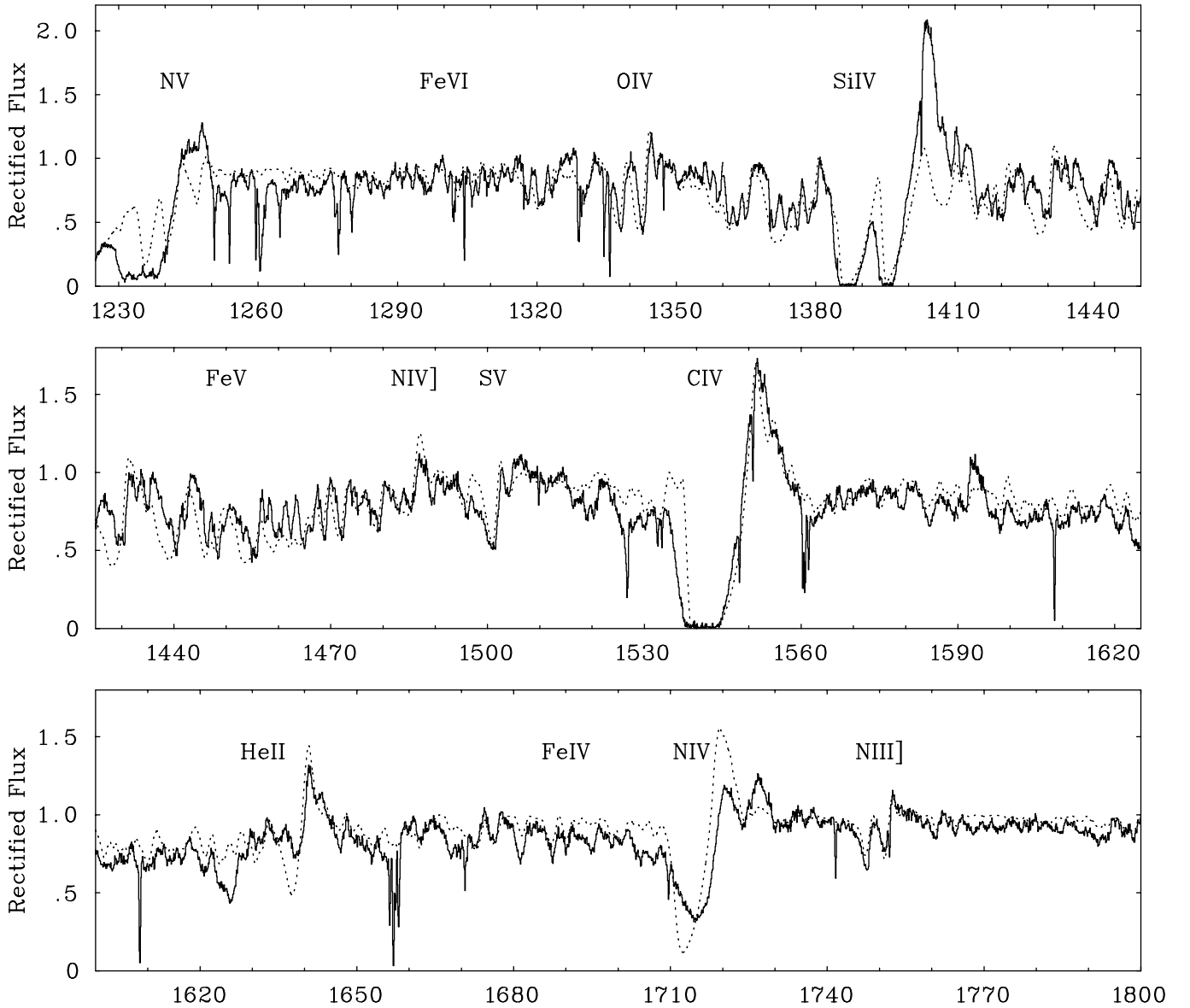


Fig. 3. Plots of selected regions of the UV spectrum of HD 153919 (solid line) and best fit model (dotted line); parameters listed in Table 1. Note that our model does not take into account the observed Raman-scattered emission lines (which are not of a photospheric origin) in the range 1400–1700 Å.

would reduce this value by a factor of ~ 2 . Derived parameters are listed in Table 1, and are in reasonable agreement with those derived by vL01 through the analysis of ultraviolet resonance lines based on the Sobolev with Exact Integration (SEI) method.

Our primary nitrogen abundance diagnostics are N III $\lambda 4634\text{--}41$ and $\lambda 4097$, which together imply $\epsilon_{\text{N}} = 9\epsilon_{\text{N},\odot}$. With this value, the very weak N III $\lambda 5320\text{--}4$ feature is well matched, but other lines in the vicinity of He II $\lambda 4542$ are somewhat too strong (likely due to an incomplete treatment of N III quartet states in our models). Carbon is somewhat more difficult to constrain, with C III $\lambda 4647\text{--}51$ well matched for $\epsilon_{\text{C}} = 1.0\epsilon_{\text{C},\odot}$. C IV $\lambda 5801\text{--}12$ is well reproduced with this value, whilst C III $\lambda 5696$ is too weak, implying a yet higher abundance. As discussed elsewhere (e.g. Hillier et al. 1998), oxygen is exceedingly difficult to constrain in mid-O

supergiants due to lack of suitable optical diagnostics. The high nitrogen overenrichment is not easily explained via single star evolution, unless carbon (and to a lesser degree oxygen) is very depleted via the CN (or ON) cycle. Crowther et al. (2002) discuss similar problems for Magellanic Cloud O supergiants.

Turning to UV comparisons, we show rectified high resolution IUE spectroscopy of HD 153919 (phase 0.15) in Fig. 3 together with synthetic spectra. Overall, agreement for He II $\lambda 1640$, C IV $\lambda 1550$ and N IV $\lambda 1718$ is reasonable, with predicted Si IV $\lambda 1393\text{--}1402$ emission too weak adopting $\epsilon_{\text{Si}} = 1.0\epsilon_{\text{Si},\odot}$. Since X-rays are not explicitly considered in this study, the shocked UV N V $\lambda 1238\text{--}42$ resonance doublet is predicted to be too weak. The sole prominent oxygen feature present in the UV (or optical) region is O IV $\lambda 1338\text{--}43$, which is reasonably well matched with $\epsilon_{\text{O}} = 0.5\epsilon_{\text{O},\odot}$, although we do not claim that this represents an accurate constraint.

Additional, powerful evidence in favour of our derived temperature is the good match between the synthetic Fe IV-V spectrum and observations, again with $\epsilon_{\text{Fe}} = 1.0\epsilon_{\text{Fe},\odot}$. Figure 2 shows good agreement with the dominant Fe V “forest” observed between $\lambda 1300$ – 1600 in HD 153919, plus the weaker Fe IV in the $\lambda 1500$ – 1800 region. Fe VI is not strongly predicted nor observed in the $\lambda 1200$ – 1400 region (see Crowther et al. 2002 for further details).

While it is possible to explain the nitrogen enrichment in terms of rotational mixing it is impossible to produce carbon enrichment via this mechanism. Any carbon produced in the helium burning layers of the star has to pass through the hydrogen burning layers before reaching the surface where it will be converted to nitrogen. Therefore, any excess carbon in HD 153919 is therefore likely to result from mass transfer from the more evolved binary component prior to SN – this will be returned to in Sect. 4.

Given the presence of a compact companion for HD 153919, it is reasonable to ask whether the assumption of spherical geometry is justified – does the X-ray flux lead to significant departures from spherical symmetry for the ionisation of the wind (which in turn could lead to modifications in the line driving force)? Hatchett & McCray (1977) suggest that the X-ray emission will lead to a reduction of moderately ionised atoms in the wind (such as Si IV and C IV). Given that the ionised zone will move with the compact object we might expect to see orbital modulation in some of the wind UV resonance lines as the ionised zone passes in front and behind the stellar disc (or from the presence of a photo-ionization wake in the system, cf. Kaper et al. 1994). However, there is no convincing evidence for orbital modulation in the UV resonance line due to the Hatchett-McCray effect (e.g. Kaper et al. 1990, 1993); the small changes in line profiles with orbital phase are instead most likely due to Raman scattering of EUV photons generated by the X-ray source (Kaper et al. 1990, 1993). Additionally, the modeling was performed on the spectrum obtained during the X-ray eclipse to further minimise any possible effects of irradiation on the stellar wind (cf. Sect. 2.1).

Using a modified 2-dimensional Sobolev Exact Integration (SEI) code vL01 analyse the UV line variability and confirm that any Strömgren sphere caused by the presence of the X-ray source is rather small, and will have a negligible effect on the ionization structure and line driving of the wind (since the wind is dense and the ionizing flux low). Equally, the Strömgren zone does not extend to the surface of the star and so should not lead to a significant degree of X-ray heating of the stellar surface.

Phase resolved continuum observations (e.g. vL01; Hammerschlag-Hensberge & Zuiderwijk 1977; van Paradijs et al. 1978) constrain orbital variability to <4 per cent in the UV and 4–8 per cent in the optical, indicating that HD 153919 shows little departure from sphericity (possibly as a result of a large mass ratio). Note that continuum emission from the stellar wind is essentially negligible at wavelengths shorter than a few microns. Therefore, the lack of significant variability cannot be attributed to emission from the outer regions of the stellar wind “shielding” a heavily perturbed stellar surface and/or inner wind from view.

The photometric variability further constrains any change in stellar temperature due to X-ray heating to less than the uncertainty in the stellar temperature derived from our NLTE modeling. Therefore, we have confidence that deviations from spherical symmetry in HD 153919 and/or the effects of X-ray irradiation are negligible for the purposes of spectroscopic modeling.

3. Mass determination for the system components

Since no X-ray pulsations have been convincingly measured for 4U1700-37 – and hence no determination of $a_x \sin i$ is possible – the orbital solution cannot be uniquely determined. However, following Heap & Corcoran (1992) and Rubin et al. (1996) we may estimate the mass of the companion using a Monte Carlo method. The mass of the companion can be calculated using a series of equations relating eclipse and orbital parameters.

The Roche lobe filling factor Ω is defined by

$$R_* = \Omega R_L \quad (1)$$

where R_* is the radius of the O-star and R_L is the Roche lobe radius which is related to the semi-major axis of the system a and the mass ratio $q(=M_{\text{ast}}/M_x)$ by

$$\frac{R_L}{a} = A + B \log q + C(\log q)^2 \quad (2)$$

and the coefficients A , B and C are

$$A = 0.398 - 0.026\Gamma^2 + 0.004\Gamma^3$$

$$B = -0.264 + 0.052\Gamma^2 - 0.015\Gamma^3$$

$$C = -0.023 - 0.005\Gamma^2$$

where Γ is the ratio of the rotational angular frequency of the companion to its orbital angular frequency (Rappaport & Joss 1983).

The radius of the O-star is related to the semimajor axis by the inclination i and eclipse semiangle θ_E by

$$\frac{R_*}{a} = \sqrt{\cos^2 i + \sin^2 i \cos^2 \theta_E} \quad (3)$$

while the companion mass function f is given by

$$M_x^3 \sin^3 i = f(M_* + M_x)^2 \quad (4)$$

and f is related to orbital parameters by

$$f = 1.038 \times 10^{-7} K_* P (1 - e^2)^{3/2} \quad (5)$$

where K_* is the radial velocity semi-amplitude in km s^{-1} , P the period in days and e the ellipticity. Finally by Kepler’s third law

$$a^3 = 75.19(1 + q)M_x P^2. \quad (6)$$

We combine these equations in a similar way to Rubin et al. (1996) to obtain

$$R_*^2 = \frac{R_L^2}{R_{La}^2} - 17.81 P^{4/3} f^{2/3} (1 + q)^2 \cos^2 \theta_E \quad (7)$$

Table 1. Stellar parameters for HD 153919 derived from the NLTE modeling described in Sect. 2.2.

Parameter	Value
$E(B - V)$	0.54 ± 0.02
T_{eff}	$35\,000 \pm 1000$ K
$\log(L_*/L_\odot)$	5.82 ± 0.07
R_*	$21.9^{+1.3}_{-0.5} R_\odot$
\dot{M}	$9.5 \times 10^{-6} M_\odot \text{ yr}^{-1}$
v_∞	1750 km s^{-1}
$\log g$	$3.45\text{--}3.55$

where $R_{La} = R_L/a$. This equation can then be solved numerically for q .

Values of various system parameters (listed in Table 2) are selected randomly either from a Gaussian distribution (if observed) or uniformly if constrained between certain values. Equation (7) is solved for q which gives a from Eq. (2) which then gives M_x from Eq. (6). Consistency can be checked by requiring $\sin i < 1$ and $i > 55$ degrees (e.g. Rubin et al. 1996).

This procedure is followed 10^6 times to gain a distribution of M_x and M_* for a considerable number of possible parameter combinations (noting that as expected there is a very strong positive correlation between the two masses). We find that $M_x = 2.44 \pm 0.27 M_\odot$. As shown by the histogram of M_x in Fig. 4 the distribution is very asymmetric beyond the 1σ limits (determined by the 16th and 84th percentile of the cumulative distribution function), with only 3.5 per cent of the sample having a mass of less than $2 M_\odot$, and *none* less than $1.65 M_\odot$ (which is significantly higher than the upper limit to the range found for binary pulsars by Thorsett & Chakrabarty 1999). We note that *none* of the 10^6 trials were rejected from inclination constraints suggesting that the range of stellar radii adopted for the modeling are unlikely to be significantly in error (which, for the fixed eclipse length, would lead to unphysical solutions for the orbital inclination).

The errors on M_x are significantly smaller than previous work (e.g. Rubin et al. 1996) due to the far more stringent limits on R_* , which constrain the orbital and eclipse parameters far more strongly. This is not surprising as the eclipse parameters are used to work out the orbital parameters and the eclipse constraints rely strongly on the O-star radius.

Figure 5 shows the O-star mass distributions around $M_* = 58 \pm 11 M_\odot$. Again the distribution is anti-symmetric with 32 per cent of trials between $50\text{--}60 M_\odot$, 26 per cent between $40\text{--}50 M_\odot$ and only 2 per cent less than $40 M_\odot$. Therefore, the mass implied for HD 153919 appears to be consistent with both that expected from its spectral classification and relevant evolutionary tracks (see Fig. 6), and that suggested by its high terminal wind velocity (Sect. 2). Additionally the $\log g$ determined from the He I and Balmer line wings (Sect. 2.2) indicates a *minimum* mass of $50 M_\odot$ (and maximum of $\sim 60 M_\odot$), again fully consistent with the results of the Monte Carlo simulation. Therefore, given the consistency between mass estimates based on spectral type, evolutionary tracks (when compared to the stellar temperature and luminosity derived from modeling), surface gravity and the Monte Carlo simulations, we have confidence that the mass of HD 153919 lies in the range $50\text{--}60 M_\odot$.

This resolves the problem that the star is undermassive by a factor of ~ 2 .

However, the mass of the compact companion is more problematic given that it is *significantly* in excess of the observed mass range for NS, but apparently considerably lower than those found for BH candidates (e.g. Fig. 7). If a minimum mass of $50 M_\odot$ is adopted for HD 153919 the minimum value of M_x that may be obtained is $1.83 M_\odot$, while for values of M_o between $50\text{--}60 M_\odot$ only 0.17 per cent of trials result in $M_x < 2 M_\odot$. This will be returned to in Sect. 5.

Recent reanalysis of spectroscopic data by Hammerschlag-Hensberge et al. (in prep.) suggests that the eccentricity of the orbit is somewhat uncertain, and that the orbital velocity curve is equally well fit by an orbit of eccentricity $e \sim 0.22 \pm 0.04$ as it is by a circular orbit. In order to address this uncertainty we modified the above equations for the more general case of an elliptical orbit and repeated the simulations with $e = 0.22 \pm 0.04$. This resulted in significantly higher masses for both components, with $M_* = 70 \pm 7 M_\odot$ and $M_x = 2.53 \pm 0.2 M_\odot$. Therefore, the mass of the O star in the case of an elliptical orbit is significantly higher than expected for an O6.5 Iaf+ star (only 0.002 per cent of the trials result in a mass $\leq 50 M_\odot$, and 5 per cent give a mass between $50\text{--}60 M_\odot$). Such high values for M_* are inconsistent with the measured $\log g$ and we note that 95 per cent of trials are rejected due to the inclination constraints, suggesting that a low eccentricity solution is more likely.

If such extreme values for M_* are adopted, the mass of the compact object is still less than that observed for the lowest mass black hole candidate known ($\sim 4.4 M_\odot$; Sect. 5) and remains significantly greater than any known neutron star. Indeed, the lowest mass estimates for both components were derived in the case of a circular orbit; therefore the value of $M_x = 2.44 \pm 0.27 M_\odot$ represents a lower limit for the mass of the compact object³, and we suggest that these results favour a low eccentricity solution for the orbit (we note that the orbital eccentricity of Vela X-1 is overestimated from optical observations when compared to the value derived from timing analysis, cf. Barziv et al. 2001).

4. Evolutionary history of 4U1700-37

The stellar parameters for both primary and compact companion determined via non-LTE modeling and Monte-Carlo simulation raise many important questions regarding the evolution of single and binary massive O stars and their ultimate post-SN fate. However, such questions are complicated by the uncertain evolution of massive stars after leaving the main sequence and the role that binarity and associated – possibly non-conservative – mass transfer plays in modifying this; for instance the time at which the hydrogen rich outer layers are lost exposing the helium core plays a critical role in determining the final pre-SN mass of the star (e.g. Brown et al. 2001 and references therein).

³ Values of $M_x < 2 M_\odot$ are only obtained when the radial velocity semi-amplitude, K_0 , is $> 2\sigma$ below the observed value, to obtain $M_x < 1.6 M_\odot$ would require K_0 to be wrong by several sigma.

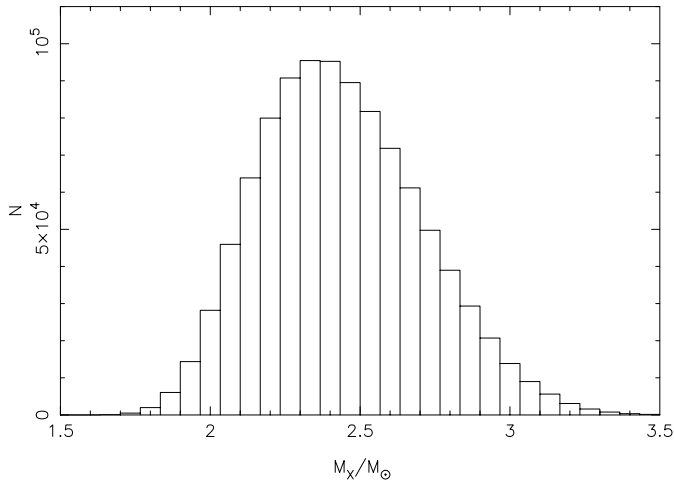


Fig. 4. Histogram of the results of the Monte Carlo simulations for the mass of the compact object in 4U1700-37. The results indicate a mass in the range of $2.44 \pm 0.27 R_{\odot}$ with only 3.5 per cent of simulations indicating masses of less than $2 M_{\odot}$, and none $< 1.65 M_{\odot}$.

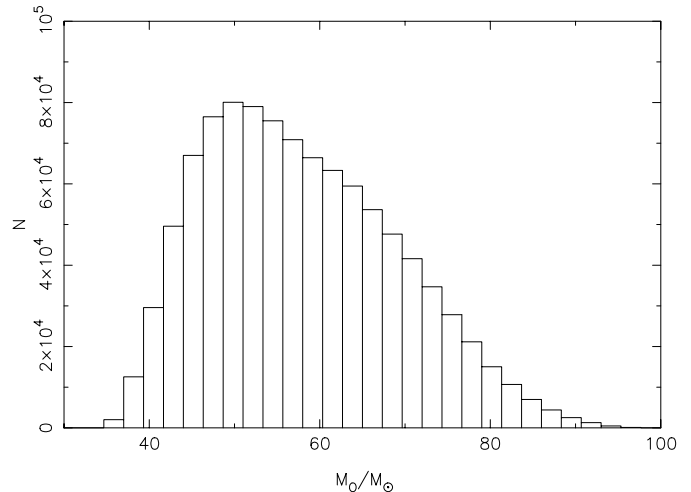


Fig. 5. Histogram of the results of the Monte Carlo simulations for the mass of the O6.5Iaf+ primary HD 153919 – the results indicate a mass in the range of $58 \pm 11 R_{\odot}$ consistent with evolutionary predictions and the mass estimated from our determination of $\log g = 3.45\text{--}3.55$ (Sect. 2.2).

Heap & Corcoran (1992) propose an initial $80 M_{\odot} + 40 M_{\odot}$ binary system with subsequent evolution via case B mass transfer⁴ after 2.6×10^6 yrs, proceeding for 10^4 yrs (via Roche-lobe overflow; RLOF). After the mass transfer the initially more massive star has lost enough material due to the combination of wind driven mass loss and the brief period of *non-conservative* RLOF to become a WR star, which subsequently explodes as a SN.

Based on their identification of the Sco OB1 association as the birthplace of HD 153919, Ankaa et al. (2001) propose a lower initial mass of the SN progenitor ($\geq 30^{+30}_{-10} M_{\odot}$) based on the turnoff mass for the proposed 6 ± 2 Myr age of Sco OB1 at the time of the supernova. Assuming *conservative* Case B mass transfer they derive an initial mass of at least $25 M_{\odot}$ and suggest the short orbital period Wolf-Rayet (WR) binary CQ Cep/HD 214419 as a possible example of the progenitor system. However they note that the assumption of conservative mass loss might be incorrect and highlight the non-conservative scenario of Wellstein & Langer (1999). Such a scenario is attractive since the loss of substantial quantities of mass and angular momentum naturally lead to short period binaries (assuming both components do not merge). However, common envelope evolution is poorly understood and therefore somewhat limits our ability to quantitatively reconstruct the pre-SN evolution of the binary.

Despite these uncertainties we can address the general evolution of the binary in some detail. Our present mass estimate for HD 153919 of $M_* = 58^{+11}_{-11} M_{\odot}$ suggests a mass for the SN progenitor of the order of $\geq 60 M_{\odot}$, at the upper range of

Table 2. Physical parameters of 4U 1700-37. Those with a \pm have a Gaussian error distribution while those without are assumed to have a uniform distribution.

Parameter	Value
R_*	$21.4\text{--}23.2 R_{\odot}$
Γ	$0.5\text{--}1.0^a$
Ω	$0.8\text{--}1.0^a$
e	0.0^b
θ_E	28.6 ± 2.1 degrees ^a
P	$3.411581 \pm 2.7 \times 10^{-5}$ days ^a
K_*	20.6 ± 1.0 km s ^{-1b}

^a Rubin et al. (1996); ^b Hammerschlag-Hensberge et al. (in prep.).

that proposed by Ankaa et al. (2001)⁵. The short orbital period of HD 153919/4U1700-37 favours non conservative evolution probably via case B mass transfer. While mass loss via the stellar wind of the SN-precursor during the WR phase will lead to a widening of the orbit, a favourable SN kick may overcome these problems.

The alternative Case C evolution appears unlikely given that the SN will occur several thousand years after the end of mass transfer/loss. This time period appears unrealistically short given that this will not allow sufficient time for the helium mantle to be removed to expose the C/O core (i.e. the star will not pass through a WC phase). Therefore the SN progenitor would have a large mass at the point of SN; for a SN progenitor with an initial mass of $60 M_{\odot}$ we might expect the mass to be of the order of $30 M_{\odot}$ (the maximum helium core mass). This implies the loss of a very large quantity of material in the SN, contradicting the estimate of Ankaa et al. (2001) that only $\sim 9 M_{\odot}$

⁴ We adopt the nomenclature used in Wellstein & Langer (1999 and references therein), with Case A, B & C evolution corresponding to mass transfer during core hydrogen burning, after core hydrogen burning but before core helium exhaustion, and after core helium burning, respectively.

⁵ We note however, that the difference in the life time of a $60 M_{\odot}$ star (3.8 Myr) and – for example – a $120 M_{\odot}$ star (3.0 Myr) is smaller (0.8 Myr) than the uncertainty in the life time of a $60 M_{\odot}$ star (1 Myr), suggesting that higher progenitor masses may be possible.

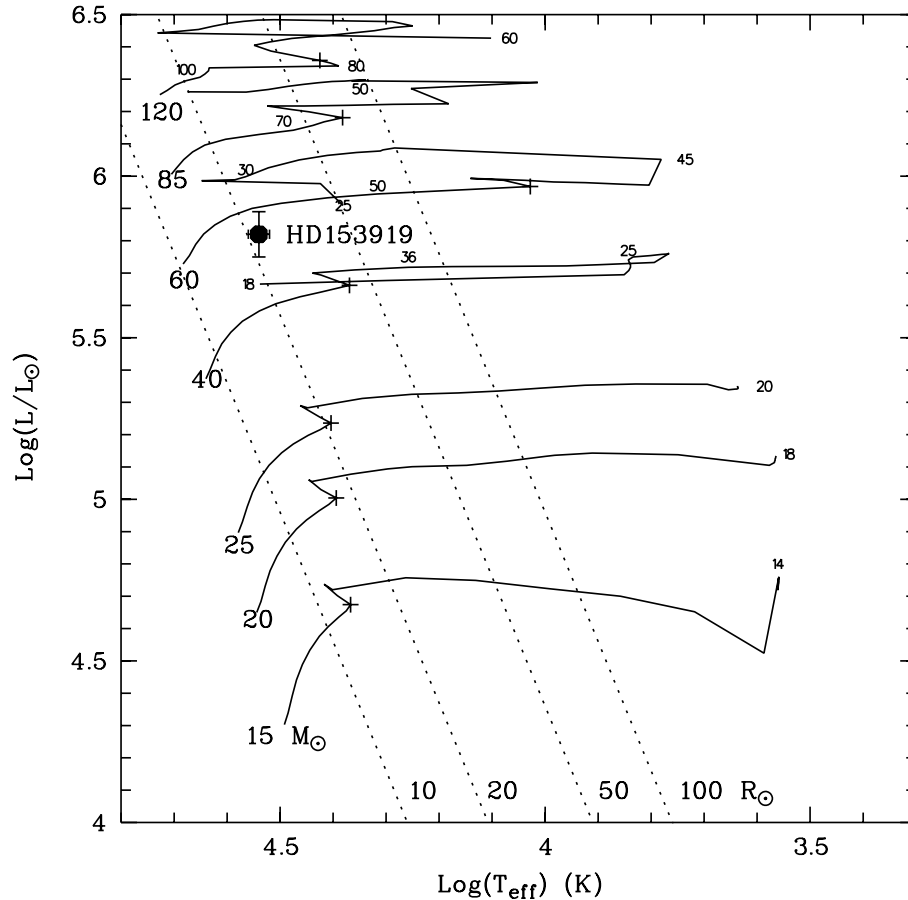


Fig. 6. The location of HD 153919 in the Hertzsprung-Russell diagram. The evolutionary tracks of Lejeune & Schaerer (2000) for stars of a given initial mass are indicated (up to the phase of core-helium burning). The numbers along the tracks show the decrease in M_* with time due to wind losses. The plus signs indicate the end of core-hydrogen burning. The diagonal dashed lines are lines of constant radius.

was lost in the SN (and we might also expect such a scenario to lead to a very high mass compact object, cf. Brown et al. 2001).

The high mass implied for the SN precursor suggests that such a star would be likely to evolve through a Luminous Blue Variable (LBV) phase rather than a Red Supergiant (RSG) phase on its way to becoming a WR star (stars with initial masses $\geq 40 M_{\odot}$ likely avoid the RSG phase). Such an evolutionary path is likely to prevent mass transfer *onto* HD 153919 via RLOF (Wellstein & Langer 1999). Significant accretion of material by HD 153919 via RLOF seems implausible in any case, as this would lead to a large orbital separation and period (Wellstein & Langer 1999). Instead, the formation and subsequent ejection of a common envelope (*despite* the SN precursor avoiding the RSG phase) and simultaneous reduction in orbital period and binary separation is suggested. Such a scenario therefore implies that the present day mass of HD 153919 forms a lower limit to the mass of the SN precursor, subject to the possible accretion of a small quantity of material directly from the wind of the SN precursor (see below).

After the ejection of the outer layers of the SN precursor we are left with a short orbital period WR+O star binary. Support for this scenario is provided by the possible overabundance of carbon (or rather the lack of significant C depletion as might be expected for CNO processed material; Sect. 2.2) in HD 153919. The carbon rich material must have originated

in the SN precursor during a carbon rich WC stage, independently suggesting a rather high initial mass for the SN precursor. Subsequent mass transfer would then have to occur via direct wind fed accretion, with the wind of the WC star impacting directly on the surface of the O star. Despite the high mass loss rate of the O star ($\dot{M} = 9.5 \times 10^{-6} M_{\odot} \text{ yr}^{-1}$; Table 2) the possibility of such accretion is suggested by hydrodynamical simulations of colliding wind binaries (Gayley et al. 1997; Dessart, Petrovic & Langer, in prep.).

We may exclude the overabundance in nitrogen originating via direct wind accretion during the WN phase of the SN precursor. For a nitrogen overabundance in HD 153919 of ~ 9 , the nitrogen mass fraction, $X_N = 0.01$, is the same value as is found in the winds of WN stars which implies that HD 153919 would have to accrete $18 M_{\odot}$ from the SN precursor during the WN phase to produce such an overabundance. Given that this is unreasonably high, we suggest that the excess nitrogen probably originated from internal, rotational mixing (nitrogen overabundances are not unusual for O stars).

Several short period WR+O star binaries are known and could provide analogues to the precursor of the present binary configuration. At present CQ Cep does not fit particularly well ($M_{\text{WN}} = 21 M_{\odot}$, $M_{\text{O9}} = 26 M_{\odot}$, $P = 1.6$ days) – in a few 10^5 yrs when the WN star has lost mass and has evolved into a lower mass WC star (and the period has lengthened) it may provide a

better model for the system. However, of the known WC+O binaries, HD 63099 ($M_{\text{WC}} = 9 M_{\odot}$, $M_{\text{O7}} = 32 M_{\odot}$, $P = 14$ days) could evolve into a HD 153919/4U1700-37 like binary if the SN kick is favourable. Other known WR+O star binaries that could form similar systems are HD 152270 ($M_{\text{WC}} = 11 M_{\odot}$, $M_{\text{O5-8}} = 29 M_{\odot}$, $P = 8.9$ days) and HD 97152 ($M_{\text{WC}} = 14 M_{\odot}$, $M_{\text{O7}} = 23 M_{\odot}$, $P = 7.9$ days); in all three cases the present mass of the WC star is $\geq 9 M_{\odot}$ as suggested for the SN precursor by Ankay et al. (2001) on the basis of the present mass of the compact companion and the current space velocity of the system. Therefore, of the six WC+O binaries with known masses (van der Hucht 2001) three are found to have parameters consistent with the presumed pre-SN stage of 4U 1700-37.

The results of the Monte-Carlo simulations suggest that the SN formed a compact object (see Sect. 5) with a mass in the range $2.44 \pm 0.27 M_{\odot}$. As massive binary models show that Case B primary stars of larger initial mass evolve to a larger final mass, and that Case A primaries end up less massive than Case B's (cf. Wellstein & Langer 1999; Wellstein et al. 2001) we can conclude that the remnants of all Case A/B primaries initially less massive than about $60 M_{\odot}$ are less massive than about $2.5 M_{\odot}$.

Theoretical predictions suggest that a $60 M_{\odot}$ star in a close binary system is capable of producing either a low or a high mass compact object depending sensitively on the wind mass loss rate adopted for such a star during its WR phase; a variation of only a factor of three in the WR mass loss rate leading to compact object masses in between 1.2 and $10 M_{\odot}$ (Fryer et al. 2002). This result shows that given the present uncertainties in WR mass loss rates, the relatively low mass found for the compact star in 4U1700-37 is not in conflict with the evolutionary scenario proposed above (and also argues for a relatively high WR mass-loss rate).

Therefore, given the low mass of the compact companion in 4U1700-37, it seems to be difficult to explain any of the (high mass) galactic black hole binaries as being produced through the Case A/B channel (cf., Portegies Zwart et al. 1997) except for those with the most massive SN-progenitors (Brown et al. 2001). Indeed, evolutionary scenarios invoking Case C mass transfer (Brown et al. 1999) seem to be required to explain the high-mass black holes in low-mass X-ray binaries.

5. The compact companion

At present mass determinations exist for 36 compact objects, of which 21 are neutron stars and the remainder black hole candidates (Fig. 7). Thorsett & Chakrabarty (1999) found that the masses of neutron stars are clustered in a remarkably narrow range (mean of $1.35 M_{\odot}$ and a standard deviation of $0.04 M_{\odot}$). However, recent analysis of Vela X-1 by Barziv et al. (2001) suggests that the pulsar has a mass of $1.87^{+0.23}_{-0.17} M_{\odot}$ ⁶, while Orosz & Kuulkers (1999) find a mass of $1.78 \pm 0.23 M_{\odot}$ for Cygnus X-2 (however Titarchuk & Shaposhnikov 2002 have

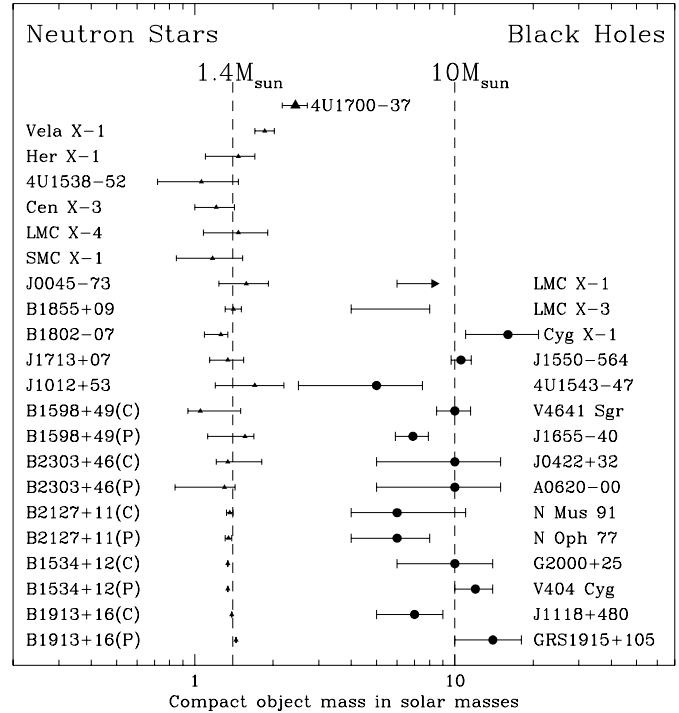


Fig. 7. Mass distribution for neutron stars and black holes (after Charles 1998). Neutron star masses are from Ash et al. (1999), Barziv et al. (2001), van Kerkwijk et al. (1995) and Thorsett & Chakrabarty (1999). Black hole masses provided by Charles (priv. comm.). Error bars for systems other than 4U1700-37 are 1 sigma errors; see Sect. 3 for a discussion of the errors associated with the mass of 4U1700-37 but note that the probability of $M < 2 M_{\odot}$ is less than 3.5 per cent, and no trials results in $M < 1.65 M_{\odot}$.

recently proposed $M = 1.44 \pm 0.06 M_{\odot}$ on the basis of Type-I X-ray bursts).

Based on assumptions about the origin of kilohertz quasi-periodic oscillations Zhang et al. (1997) suggest that several LMXBs may also contain massive ($\sim 2 M_{\odot}$) neutron stars, resulting from the accretion of substantial amounts of material over long (10^8 yrs) periods of time. However their putative descendants, radio pulsar+white dwarf binaries, provide no evidence for massive neutron stars (Barziv et al. 2001). The same is true for the Be/X-ray binaries, which have evolved from lower mass systems than the OB-supergiant HMXBs. Only in the latter systems evidence has been found for massive neutron stars and black hole candidates.

Masses for a number of black hole candidates have also been determined; lower limits to their masses comfortably exceed $3 M_{\odot}$. Indeed several objects appear to have masses $\geq 10 M_{\odot}$ (e.g. $14 \pm 4 M_{\odot}$ for GRS 1915+105; Greiner et al. 2001), with most typically $\geq 6 M_{\odot}$. At present the binary system with the lowest mass candidate black hole is Nova Vel ($4.4 M_{\odot}$; Filippenko et al. 1999).

Given that the mass of the compact object in 4U1700-37 lies outside the present observational range for both neutron stars and candidate black holes, is it possible to increase/decrease the mass of the compact object such that it is consistent with either type of object? For the case of a circular orbit we find *no* solutions consistent with $M_x \gtrsim 4.4 M_{\odot}$.

⁶ Systematic excursions in the radial velocity curve for this system complicate this determination and prevent an *unambiguous* confirmation of the mass estimate for the neutron star (Barziv et al. 2001).

Very eccentric orbital solutions do allow values of M_x in this range although we note there is no physical motivation for them. Such solutions imply values of M_0 greatly in excess of $100 M_\odot$, well above current evolutionary predictions for the mass of an O6.5 Iaf+ star. Stars with masses in excess of $100 M_\odot$ are instead expected to evolve to H depleted WR stars via a H rich pseudo-WNL phase where their powerful stellar winds mimic the spectra of more (chemically) evolved stars of lower masses.

Such a large mass would also be inconsistent with the constraints imposed by the surface gravity (Sect. 2.2) and the relationship between stellar mass and the terminal wind velocity. Finally the result would imply that even very massive stars (given that the initial mass of the SN progenitor had to be significantly in excess of the present mass of HD 153919) leave relatively low mass remnants post supernova, presenting significant problems for the origin of heavy ($>10 M_\odot$) black holes such as e.g. Cyg X-1. Therefore we conclude that M_x appears to be inconsistent with the range of masses of *known* black hole candidates.

Given the stringent lower limits derived in Sect. 3 it also appears difficult to bring the mass of the compact object into line with the range of masses found by Thorsett & Chakraborty (1999). Inspection of the evolutionary tracks in Fig. 6 suggest that stars with initial masses of the order of $60 M_\odot$ initially evolve redwards before returning bluewards after undergoing significant mass loss, most likely during an LBV phase. While we note that the behaviour of stars in this short lived phase is very uncertain it is unlikely that we could be observing HD 153919 after such an excursion, since we would expect significant chemical enrichment – the H rich mantle having been lost – which is not observed. Likewise, the mass constraint imposed by the determination of the surface gravity also appears to exclude this scenario.

Furthermore, such a low value for M_0 and M_x would reintroduce the problem of HD 153919 being undermassive for its spectral type by a factor ≥ 2 . While the primaries in some HMXB systems are found to be undermassive (e.g. Cen X-3 and LMC X-4; Kaper 2001) this is attributed to mass loss via RLOF – wind fed systems do not show this effect (Kaper 2001). Given that 4U1700-37 is currently a wind fed system and is yet to evolve into a RLOF system this could not explain such a mass discrepancy. Indeed, given the evolutionary constraints imposed by the present orbital period it is likely that no significant mass transfer has occurred onto HD 153919 during its lifetime, and it will have evolved as if it were an isolated star.

5.1. Implications of an intermediate mass

If we accept $M_x = 2.44 \pm 0.27 M_\odot$ – as implied by the simulations – the nature of the compact companion remains uncertain. Conflicting claims as to the nature of the object have been made on the basis of the X-ray spectrum of 4U1700-37 (Sect. 1). While we cannot discriminate between the twin possibilities of massive neutron star or low mass black hole from our present measurements we note that consideration of the masses of *both* components of the binary appear to exclude the possibility that

stars with masses of $\sim 60 M_\odot$ can produce $5\text{--}10 M_\odot$ black holes via case A or B evolution.

If the compact object in 4U1700-37 is a black hole it confirms Brown et al.’s prediction of the existence of “low mass black holes” (based on their “soft” equation of state, Brown et al. 1996), while if the object is a neutron star the high mass would severely constrain the equation of state of matter at supra-nuclear densities.

The relationship between the mass of a neutron star and its central density is calculated by integration of the Tolman-Oppenheimer-Volkoff (TOV) equation (Oppenheimer & Volkoff 1939) which is the relativistic expression for hydrostatic equilibrium. In order to perform the integration it is necessary to understand the equation of state of the degenerate nuclear matter in the star.

Because of their non-perturbative nature, strong interactions between nuclei are extremely difficult to calculate even under normal conditions. However, there are several models of the internuclear potential in the literature which have achieved much success in modelling nuclei e.g. Stoks et al. (1994), Wiringa et al. (1995) and Machleidt et al. (1996). One of the most successful and up to date of these models has been applied to the neutron star equation of state by Akmal et al. (1998) yielding a maximum mass of between 2.2 and $2.4 M_\odot$ for a neutron star made completely of normal nuclear matter.

There is also the possibility of a QCD phase transition occurring in the centre of the neutron star. The large chemical potential has a similar effect to a large temperature on the QCD coupling constant. Consequently the interquark coupling can be reduced to the point where deconfinement occurs and nuclei dissolve into quark matter. The presence of quark matter has the effect of softening the equation of state which leads to a lower possible maximum mass for the neutron star. The energy scale at which deconfinement occurs can be parameterised by the QCD bag constant B , a phenomenological parameter representing the difference in energy density between the vacua of hadronic and quark matter ($B \approx 120\text{--}200 \text{ MeV fm}^{-3}$). Inclusion of a phase transition to such a mixed state reduces the maximum mass of the neutron star to $\sim 2 M_\odot$ for $B = 200 \text{ MeV fm}^{-3}$ and $\sim 1.9 M_\odot$ for $B = 122 \text{ MeV fm}^{-3}$ (Akmal et al. 1998)⁷.

If the neutron is rotating rapidly, the TOV equation ceases to be a valid approximation and one must drop the assumption of spherical symmetry in the metric. The effect of the rotation will increase the allowed mass of the neutron star as one might expect, but it is shown (Heiselberg & Hjorth-Jensen 1999) that even with rotation one cannot obtain a neutron star with a mass much higher than those listed above without using an equation of state so stiff that the sound speed in the neutron-star interior becomes superluminal.

To summarize this subsection, state of the art models for nuclear equations of state which include the effects of three nucleon interactions marginally allow the existence of a $2.4 M_\odot$

⁷ Hyperons such as Δ , Σ and Λ may also be produced at high density and it is thought that their presence will also soften the equation of state and reduce the overall permitted neutron star mass (Heiselberg & Hjorth-Jensen 1999).

neutron star. However, the existence of such a star would place severe constraints upon the onset of new physics at high hadronic densities. For instance, in the model where a quark matter core is expected to develop, the bag constant B would have to be considerably larger than 200 MeV fm^{-3} in order for such a star to be viable.

6. Summary

We have performed a sophisticated NLTE analysis on the O6.5 Iaf+ star HD 153919, the primary of the HMXB 4U1700-37 and used the results to constrain the masses of both components of the system via a Monte Carlo simulation. Our NLTE model atmosphere analysis leads to parameters for HD 153919 of $\log(L_*/L_\odot) = 5.82 \pm 0.07$, $T_{\text{eff}} = 35\,000 \pm 1000 \text{ K}$, $R_* = 21.9_{-0.5}^{+1.3} R_\odot$, $\dot{M} = 9.5 \times 10^{-6} M_\odot \text{ yr}^{-1}$, and an overabundance of nitrogen and possibly carbon over solar metallicities. Combined with the short orbital period of the system this implies a common envelope phase of pre-SN evolution – *despite the mass of the SN progenitor apparently precluding a RSG phase* – leading to the formation of a close WC+O star binary, with the carbon enrichment of HD 153919 a result of the impact of the stellar wind of the WC star on the surface of the O star.

The Monte Carlo simulations result in masses for the O star and compact object of $M_* = 58 \pm 11 M_\odot$ and $M_x = 2.44 \pm 0.27 M_\odot$, with none of the 10^6 trials resulting in $M_x \leq 1.65 M_\odot$, while only 3.5 per cent of the trials result in $M_x \leq 2 M_\odot$. Given that no significant mass transfer via RLOF has occurred this implies that the initial mass of the SN precursor must have been $\geq 60 M_\odot$. Thus even very massive stars can effectively “melt down” to leave rather low mass post-SN remnants. Equally, the masses of both components imply that it is impossible for stars of $\sim 60 M_\odot$ to leave 5–10 M_\odot remnants via Case A or B evolution, suggesting that most high mass black holes are instead formed via Case C mass transfer.

The mass of the compact object is found to lie in between the range of masses observed for neutron stars and black holes. Given that M_* and M_x are strongly correlated, forcing consistency between M_x and either type of object results in significant discrepancies between M_* and evolutionary predictions for the mass of HD 153919.

In order to produce consistency with the range of masses observed for neutron stars the O star has to be significantly undermassive for its spectral type and luminosity class. While theoretical evolutionary tracks for massive ($\geq 60 M_\odot$) stars suggest that after a redwards excursion the star will evolve bluewards again with a substantially reduced mass, such a star would show significant chemical enrichment (and H depletion) which is not observed. Equally, the surface gravity determined from modeling excludes such an anomalously low mass.

Forcing consistency between M_x and the masses of known black hole candidates ($M_x \geq 4.4 M_\odot$) results in $M_* \geq 100 M_\odot$. Stars of such extreme masses are not expected to go through an O supergiant phase, rather evolving into H depleted WR stars via a H-rich pseudo WR phase, where their high mass loss rate simulates the spectrum of a WR star. Once again, the constraint implied by the surface gravity also appears to exclude this possibility.

We are therefore left with the conclusion that no solution is fully consistent with present expectations for stellar evolution and the chemical abundances and surface gravity of HD 153919. If the compact object has a mass consistent with the observed range of neutron star masses, the O star is significantly undermassive, while if it consistent with the lower limit to black hole masses the O star is overmassive by a similar (or larger) factor. Finally if – as the Monte Carlo analysis implies – the probable mass of the O star is consistent with evolutionary predictions and the measured surface gravity, the mass of the compact object lies in between the two alternatives.

While our results do not allow us to distinguish between a massive neutron star or a low mass black hole, the existence of a neutron star of mass in the mass range $2.44 \pm 0.27 M_\odot$ would significantly constrain the high density nuclear equation of state and provide details about the QCD phase transition complementary to information about the temperature induced transition which will be obtained at RHIC and LHC. Phenomena which might occur deep in the star such as the appearance of hyperons or a quark matter core would be strongly constrained as the existence of these phases might result in an equation of state too soft to support such a high mass star.

Acknowledgements. This paper is partially based on observations collected at the European Southern Observatory, Chile. The United Kingdom Infrared Telescope is operated by the Joint Astronomy Centre on behalf of the U.K. Particle Physics and Astronomy Research Council. JSC, SPG & CB gratefully acknowledge PPARC funding. LK is supported by a fellowship of the Royal Academy of Arts and Sciences in The Netherlands. MF is supported by the FNRS and was helped by conversations with Nicolas Borghini; we also thank John Porter, Marten van Kerkwijk and Phil Charles for their helpful comments.

References

- Akmal, A., Pandharipande, V. R., & Ravenhall, D. G. 1998, Phys. Rev., C58, 1804
- Ankay, A., Kaper, L., De Bruijne, J. H. J., et al. 2001, A&A, 370, 170
- Ash, T. D. C., Reynolds, A. P., Roche, P., et al. 1999, MNRAS, 307, 357
- Balona, L. A., & Laney, C. D. 1995, MNRAS, 276, 627
- Barziv, O., Kaper, L., van Kerkwijk, M. H., Telting, J. H., & van Paradijs, J. 2001, A&A, 377, 925
- Bohannan, B., & Crowther, P. A. 1999, ApJ, 511, 374
- Bolton, C. T., & Herbst, W. 1976, AJ, 81, 339
- Brown, G. E., Weingartner, J. C., & Wijers Ralph, A. M. J. 1996, ApJ, 463, 297
- Brown, G. E., Lee, C.-H., & Bethe Hans, A. 1999, New Astron., 4, 313
- Brown, G. E., Heger, A., Langer, N., et al. 2001, New Astron., 6, 457
- Charles, P. A. 1998, in Theory of Black Hole Accretion Disks, ed. M. Abramowicz, G. Bjornsson, & J. Pringle, CUP, 1
- Conti, P. S. 1978, A&A, 63, 255
- Crowther, P. A., & Bohannan, B. 1997, A&A, 317, 532
- Crowther, P. A., Hillier, D. J., Evans, C. J., et al. 2002, ApJ, 579, in press [astro-ph/0206257]
- Filippenko, A. V., Leonard, D. C., Matheson, T., et al. 1999, PASP, 111, 969
- Fryer, et al. 2002, ApJ, in press
- Gayley, K. G., Owocki, S. P., & Cranmer, S. R. 1997, ApJ, 475, 786

- Giacconi, R. 1973, *ApJ*, 181, L43
- Glendenning, N. K. 2001, *Phys. Rep.*, 342, 393
- Greiner, J., Cuby, J. G., & McCaughrean, M. J. 2001, *Nature*, 414, 522
- Hammerschlag-Hensberge, G., & Zuiderwijk, E. J. 1977, *A&A*, 54, 543
- Hatchett, S., & McCray, R. 1977, *ApJ*, 211, 522
- Heap, S. R., & Corcoran, M. F. 1992, *ApJ*, 387, 340 (HC92)
- Heiselberg, H., & Hjorth-Jensen, M. 2000, *Phys. Rep.*, 328, 237
- Hillier, D. J., & Miller, D. L. 1998, *ApJ*, 496, 407
- Hillier, D. J., Davidson, K., Ishibashi, K., & Gull, T. 2001, *ApJ*, 553, 837
- Hillier, D. J., Lanz, T., Heap, S. R., et al. 2002, *ApJ*, submitted
- Howarth, I., & Prinja, R. 1989, *ApJ*, 69, 527
- Hutchings, J. B. 1976, *ApJ*, 203, 438
- Jones, C., Forman, W., Tananbaum, H., et al. 1973, *ApJ*, 181, L43
- Howarth, I. D., Siebert, K. W., Hussain, G. A. J., & Prinja, R. K. 1997, *MNRAS*, 284, 265
- Kaper, L., Hammerschlag-Hensberge, G., & Takens, R. J. 1990, *Nature*, 347, 652
- Kaper, L., Hammerschlag-Hensberge, G., & van Loon, J. Th. 1993, *A&A*, 279, 485
- Kaper, L., Hammerschlag-Hensberge, G., & Zuiderwijk, E. J. 1994, *A&A*, 289, 846
- Kaper, L., Trams, N. R., Barr, P., van Loon, J. Th., & Waters, L. B. F. M. 1997, *Ap&SS*, 255, 199
- Kaper, L. 2001, in *Proc. The influence of binaries on stellar population studies*, ed. D. Vanbeveren (*Astr. and Space Science Lib.*, Kluwer Acad. Pub.), 125
- Konig, M., & Maisack, M. 1997, *A&AS*, 327, L33
- Lejeune, T., & Schaerer, D. 2001, *A&A*, 366, 538
- Machleidt, R., Sammaruca, F., & Song, Y. 1996, *Phys. Rev.*, C53, 1483
- Miller, M. C., Lamb, F. K., & Psaltis, D. 1998, *ApJ*, 508, 791
- Oppenheimer, J. R., & Volkoff, G. M. 1939, *Phys. Rev.*, 55, 374
- Orosz, J. A., & Kuulkers, E. 1999, *MNRAS*, 305, 132
- Portegies Zwart, S. F., Verbunt, F., & Ergma, E. 1997, *A&A*, 321, 207
- Rappaport, S. A., & Joss, P. C. 1983, in *Accretion-driven Stellar X-ray Sources*, ed. W. H. G. Lewin, & E. P. J. van den Heuvel (Cambridge; Cambridge University Press), 1
- Reynolds, A. P., Owens, A., Kaper, L., Parmar, A. N., & Segreto, A. 1999, *A&A*, 349, 873
- Rubin, B. C., Finger, M. H., Hasman, B. A., et al. 1996, *ApJ*, 459, 259 (R96)
- Schmidt-Kaler, Th. 1982, in *Landolt-Börnstein, Group VI, vol. 2b*, ed. K. Schaifers, & H. H. Voigt (Springer-Verlag)
- Srinivasan, G. 2001, in *Proc. Black Holes in Binaries and Galactic Nuclei*, ed. L. Kaper, E. P. J. van den Heuvel, & P. A. Woudt (*ESO Astr. Symp.*, Springer), 45
- Stoks, V. G. J., Klomp, R. A. M., Terheggen, C. P. F., & de Swart, J. J. 1994, *Phys. Rev.*, C49, 2950
- Sung, H., Bessell, M. S., & Lee, S.-W. 1998, *AJ*, 115, 734
- Thorsett, S. E., & Chakrabarty, D. 1999, *ApJ*, 512, 288
- Titarchuk, L., & Shaposhnikov, N. 2002, *ApJL*, in press [[astro-ph/0203432](#)]
- van Kerkwijk, M. H., van Paradijs, J., & Zuiderwijk, E. J. 1995, *A&A*, 303, 497
- van der Hucht, K. A. 2001, *NewAR*, 45, 135
- van Kerkwijk, M. H. 2000, in *Proc. ESO Workshop on Black Holes in Binaries and Galactic Nuclei, Garching (Sep. 1999)*, ed. L. Kaper, E. P. J. van den Heuvel, & P. A. Woudt (Springer-Verlag)
- van Loon, J. Th., Kaper, L., Hammerschlag-Hensberge 2001, *A&A*, 375, 498
- van Paradijs, J., Hammerschlag-Hensberge, G., & Zuiderwijk, E. J. 1978, *A&AS*, 31, 189.
- Wellstein, S., & Langer, N. 1999, *A&A*, 350, 148
- Wellstein, S., Langer, N., & Braun, H. 2001, *A&A*, 369, 939
- Wiringa, R. B., Stoks, V. G. J., & Schiavilla, R. 1995, *Phys. Rev. C* 51, 38
- Wolff, S. C., & Morrison, N. D. 1974, *ApJ*, 187, 69
- Zhang, W., Strohmayer, T. E., & Swank, J. H. 1997, *ApJ*, 482, L167